A Simulation of Ignition Thresholds for Low Voltage Electrical Contact Arcs in a Hydrogen-Air Mixture

Rajiv Shekhar[a,b], Carsten Uber[a], and Udo Gerlach[a]

[a]Physikalisch-Technische Bundesanstalt (PTB), Bundesallee 100, Braunschweig, Germany
[b]The University of Queensland, Brisbane, Australia

1 Introduction

The contact arc is a transient electrical discharge which occurs due to the motion of energised electrodes, such as the opening and closing of electrical contacts. This type of discharge is an important ignition source in the field of explosion safety, specifically concerning the use of electrical equipment where flammable atmospheres may arise. Although several practical measures exist for managing this risk [1], many are reliant on empirical data and procedures which are difficult to reproduce and verify. Through modelling and simulation, it is hoped that a more fundamental understanding of the contact arc's properties as an ignition source can be developed, paving the way for a more reliable and scientifically justifiable approach.

The contact arc has several characteristics that distinguish it from better know arc discharges and high voltage sparks. These include relatively low voltages (up to 50 V) and currents (usually < 1 A). Another important defining characteristic is the the duration of the discharge, which can range from 30 μs up to several milliseconds, as well as the variation of size and power output over this duration.

This study examines the relationship between these transient energy deposition characteristics, their associated losses, and ignition thresholds, using a three dimensional reactive flow simulation coupled with an empirical approximation of the discharge. Two common characteristic values, namely the minimum ignition energy and minimum ignition kernel radius, are estimated for different combinations of source parameters. Simulation results are also compared to a classical one dimensional theory.

2 Problem Definition

The problem is based on a reference electrical contact scenario and flammable gas mixture prescribed by an industry standard for explosion safety [1]. This scenario occurs in an empirical testing device defined by the standard. The arrangement and indicative dimensions of the electrodes are described in figure 1.

Correspondence to: rajiv.shekhar@ptb.de

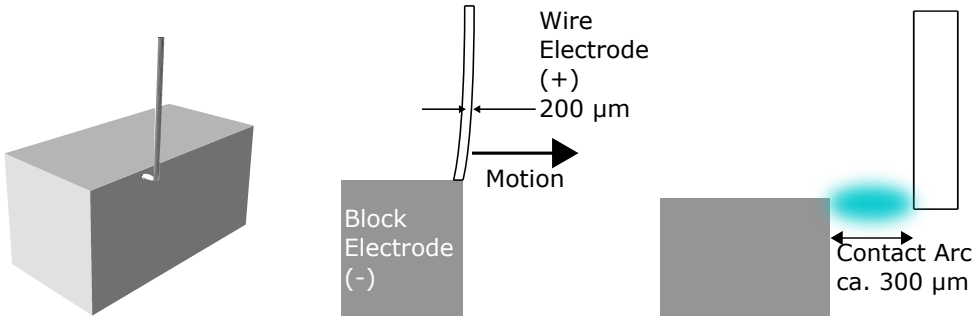

Figure 1: Overview of electrode geometry and development of contact arc

A tungsten wire and cadmium block form the positive and negative electrodes respectively. The wire is actuated such that it slides along the surface of the block. This movement causes contact arc discharges at various points, as contact is intermittently made and broken. This study focuses on one particular scenario – the discharge which forms as the wire leaves the edge of the block. This is often referred to as a "break spark". The exact process by which the discharge forms is complex, and depends on many factors including the surface conditions on the electrodes. Likewise, properties of the resulting plasma are uncertain, and are the subject of current research [2]. The plasma is also strongly suspected to be non-thermal, on account of the time, length and energy scales involved, but this is yet to be proven.

The contact arc is created in a mixture of 21% hydrogen in air at atmospheric pressure. Depending on several characteristics, including the overall energy, transient power dissipation and geometry, the contact arc may ignite the mixture. These characteristics are also dependent on one another as per the physics of the contact arc [2].

3 Simulation Overview

The OpenFOAM based simulation model of [3] is used, which solves the conservation equations for mass, momentum, energy, species in three dimensions. Chemistry is modelled by the kinetic mechanism of [4]. Fickian and thermal diffusion are included, and radiation is neglected. The geometry and gas composition of the problem space follows that of section 2, except that the moving wire electrode is omitted. An initial temperature of 300 K is assumed. A computation region up to 3 mm from the point at which the wire leaves the edge is considered. A first approximation to model heat transfer through the block electrode is obtained by solving a 1-D heat equation on its surface in the perpendicular direction.

The contact arc discharge appears as an empirical source term in the energy conservation equation. The electrical properties of the discharge are given by equation 1. This is based on a classical equation for stable arcs (modified to incorporate moving electrodes), with parameters σ and α fitted from transient voltage and current measurements, and voltage v_{fall} being a property of the contact materials [5].Variables u_{arc}, i_{arc} and t_{end} are the wire electrode speed, current (both constant) and duration of the contact arc. In practice, the contact arc is specified in terms of t_{end}, i_{arc} and $v(t_{\mathrm{end}})$, these being directly observable from electrical measurements.

The source term is given by equation 2. Total power is expressed as a product of current and voltage, with v_{fall} subtracted as it occurs very close to (or within) the electrode surface and therefore contributes negligibly to power dissipation in the gas [2]. This total power is spatially distributed in a cylindrically

symmetric manner. The distribution is linear along the length of the cylinder and Gaussian in the radial direction, with vectors $\mathbf{r}$ and $\hat{\mathbf{r_0}}$ representing the spatial coordinate and axis direction respectively. This Gaussian distribution relies on another empirical parameter σ, which is determined using intensity line profiles from high speed images of the discharge [5].

$$v(t) = v_{\text{fall}} + \alpha u_{\text{arc}} t \left(1 + \frac{\beta}{i_{\text{arc}}^n}\right) \quad ; \quad 0 \leq t \leq t_{\text{end}} \tag{1}$$

$$q_h = \frac{(v(t) - v_{\text{fall}}) i_{\text{arc}}}{\sigma^2 2\pi} \exp\left[-\frac{|\mathbf{r} - (\mathbf{r} \cdot \hat{\mathbf{r_0}})\hat{\mathbf{r_0}}|^2}{2\sigma^2}\right] \quad ; \quad 0 \leq \mathbf{r} \cdot \hat{\mathbf{r_0}} \leq u_{\text{arc}} t, \quad 0 \leq t \leq t_{\text{end}} \tag{2}$$

4 Results

The ignition thresholds are examined by running simulations for different combinations of the source parameters noted in section 3. Two cases are studied here, each corresponding to chosen values for t_{end} and $v(t_{\text{end}})$. For each case, values of i_{arc} are stepped through until an ignition is observed. For the purposes of the analysis that follows, the ignition kernel boundary is defined as the thermal isosurface at 732 K. This value is chosen by simulating a steady 1-D planar flame in an identical gas mixture, then finding where the maximum of temperature gradient occurs. The thermal isosurface is calculated from the 3-D temperature field as shown in figure 2.

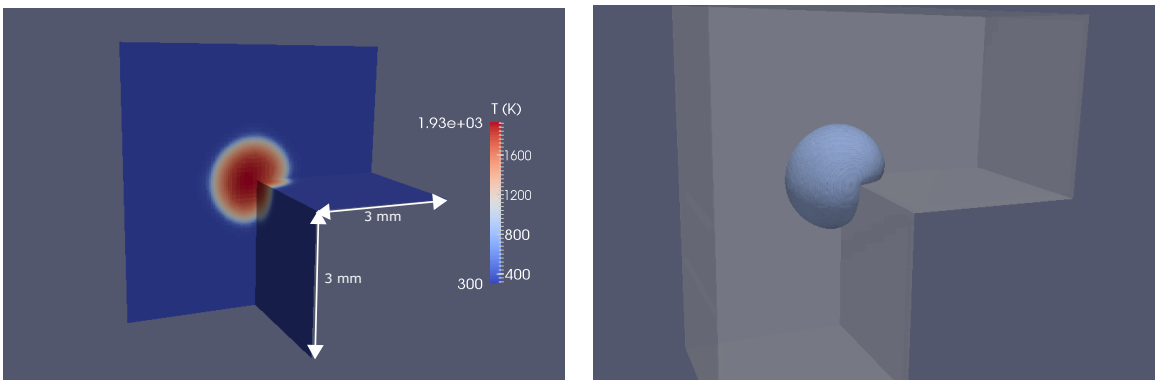

Figure 2: Left: Example of 3-D temperature field output. Right: Corresponding isosurface of 723 K

The ignition kernel volume is then defined as the volume enclosed by this isosurface. By assuming a "three-quarter sphere" geometry for the ignition kernel, an equivalent radius can be defined as $r_{eq} = \sqrt[3]{V/\pi}$, where V is the ignition kernel volume. The value of the equivalent radius over time can be plotted for each of the simulated cases, demonstrating either the extinction of the ignition kernel, or its development into a propagating flame. Additionally, the energy balance is depicted by plotting convection, total conduction, and electrode conduction losses from the kernel together with the source terms, namely input power and chemical heat release. Here, the input power from the contact arc can be defined based on equation 1, as:

$$P_{\text{arc}}(t) = \frac{t}{t_{\text{end}}} (v(t) - v_{\text{fall}}) i_{\text{arc}} \quad ; \quad 0 \leq t \leq t_{\text{end}} \tag{3}$$

Total input energy is then the integral of equation 3 from 0 to t_{end}.

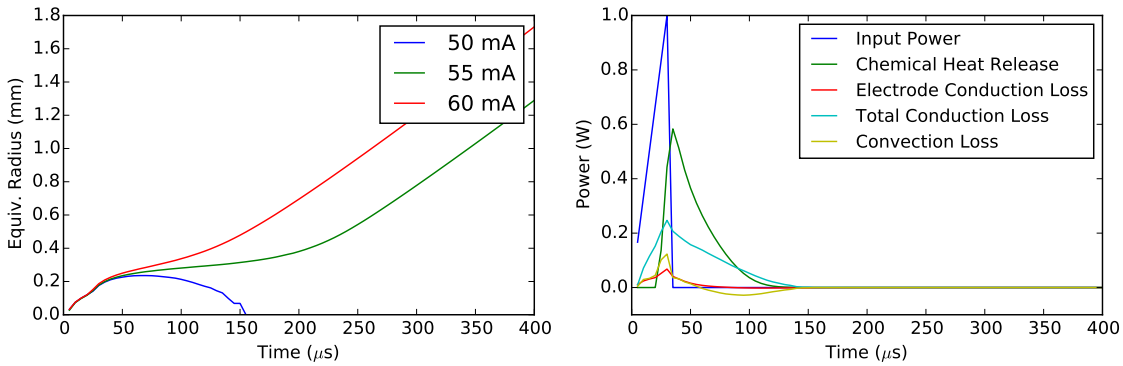

Figure 3: Simulation case 1. Left: Equivalent ignition kernel radius for various i_{arc} values. Right: Comparison of power source and loss terms for i_{arc}=50 mA

4.1 Case 1: $v(t_{\mathrm{end}})$ = 30 V, t_{end} = 30 μs

For this case, i_{arc} values of 50, 55, and 60 mA are simulated. These correspond to input energies of 15.1, 16.7 and 18.1 μJ. Values for r_{eq} vs. time are compared in figure 3. The two greater i_{arc} values result in a propagating flame, indicating that the minimum ignition energy lies between 15.1 and 16.7 μJ. In the unsuccessfully ignited case, the kernel reaches an equivalent radius of 235 μm. This can be considered as an estimate of the minimum ignition kernel radius required for ignition. The energy balance for this case is also plotted in 3. Here, the primary loss mechanism appears to be conduction, with minor roles played by convection and the electrode losses. A sign change in convection occurs at the point where the kernel begins to shrink.

4.2 Case 2: $v(t_{\mathrm{end}})$ = 30 V, t_{end} = 100 μs

For the second case, i_{arc} values of 15, 20, and 25 mA are simulated, corresponding to input energies of 15.1, 20.2 and 25.3 μJ respectively. Equivalent kernel radii are compared in figure 4, showing that only the last of these simulated i_{arc} values results in a propagating flame. The minimum ignition energy is slightly higher in this case, with a value between 20.2 and 25.3 μJ. The minimum radius estimated from the 20 mA case is also somewhat higher, at 286 μm. The energy balance for the simulation i_{arc}=20 mA shows similar trends to the previous case.

5 Discussion

An insight into the ignition threshold can be gained by considering a classical theory of 1-D spherical flames. Using a simplified system consisting of only diffusive mass and energy transport, as well a single step chemical reaction, the existence of a stationary flame ball can be shown [6]. This is an ignition kernel of a radius where energy sources and losses are perfectly balanced, and a perturbation can cause either transition to an outwardly propagating flame or extinction. The radius of the stationary flameball may therefore be comparable to the minimum ignition kernel radius observed in the simulations of section 4.

To apply this theory to the scenario of sections 2 and 3, several equivalent flame parameters must be calculated, shown in table 1. The adiabatic flame temperature T_{ad} is determined from a steady planar 1-D flame

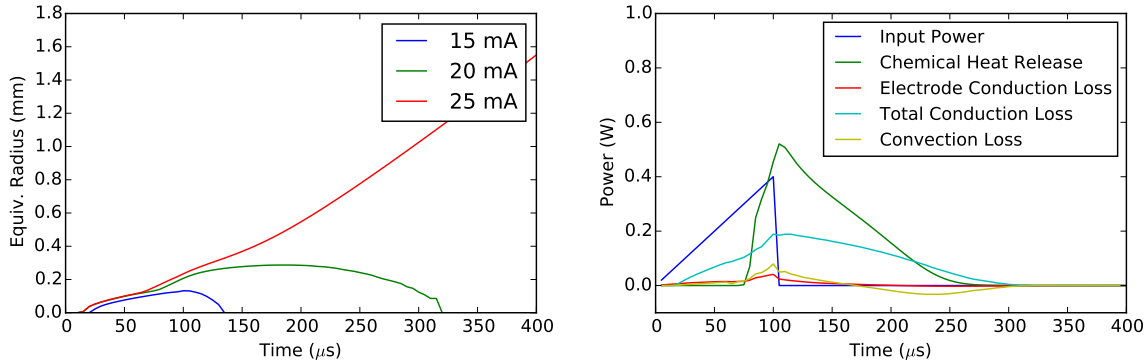

Figure 4: Simulation case 2. Left: Equivalent ignition kernel radius for various i_{arc} values. Right: Comparison of power source and loss terms for i_{arc}=20 mA

calculation using the Cantera software package [7]. The laminar flame thickness δ_T is calculated from the temperature gradient based definition, and the dimensionless activation energy $\beta = E_a/(RT_{\mathrm{ad}})$ is calculated by perturbing this 1-D flame, as per the procedure of [8]. An equivalent Lewis number Le is calculated as a weighted average of the fuel and oxidiser Lewis numbers, as per [9]. $\sigma_e = T_0/T_{\mathrm{ad}}$ and $Z = \beta(1-\sigma_e)$ are the expansion ratio and Zeldovich number respectively.

Based on these parameters, the stationary flameball radius can be calculated, according to equation 4 [6], as $r_{fb} = 146$ μm. This is somewhat smaller, although comparable in order of magnitude, to the minimum radii noted in section 4. The discrepancy is likely due to the non-spherical geometry of the real problem (and the associated inaccuracies of the integral approach taken here), but may also be partially the result of transients and minor loss mechanisms and not considered by the classical theory.

$$r_{fb} = \frac{\delta_T}{Le}\exp\left[-\frac{Z}{2}\frac{1-Le}{1-\sigma_e(1-Le)}\right] \tag{4}$$

Table 1: Equivalent flame parameters

Parameter	Value	Unit
T_{ad}	1897	K
δ_T	353	μm
β	8.18	–
Le	0.63	–
Z	6.88	–

The classical theory, of course, cannot explain the apparent difference in minimum ignition kernel radius with different t_{end} values. Although a physical explanation for this difference would require more investigation, some qualitative speculation is still possible. The energy balances of figures 3 and 4 indicate that the early phase of kernel expansion is controlled primarily by conduction loss and input power. It can also be observed that increasing t_{end} has two effects, namely, the delaying of chemical heat release, and a reduction in the heat conduction rate. A larger minimum ignition kernel radius in the case of greater t_{end} could be explained by the former of these effects being more pronounced than the latter. In other words, the longer ignition delay time is not completely compensated by a reduced thermal conduction driven kernel expansion speed, leading to a larger kernel at the point of ignition.

6 Conclusions

This brief investigation demonstrates the effect of a source parameter variation on simulated ignition thresholds for the contact arc discharge. Increasing the duration of the discharge was found to increase not only the minimum ignition energy, but also the minimum ignition kernel radius required to establish a propagating flame. Additionally the ignition process was found to be primarily governed by transient interactions between energy input, chemical heat release and conductive loss.

The long term goal of this work is the development of a simplified model to predict trends of ignition limits with variations in contact arc parameters. This will require a detailed sensitivity analysis with variations in the source parameters. and would ideally result in the formulation of a characteristic ignition limiting value that is invariant with source parameter changes.

References

[1] IEC, "IEC 60079-11 explosive atmospheres - part 11: Equipment protection by intrinsic safety," 2011.

[2] C. Uber, R. Shekhar, and L. Koenders, "Experimental investigation of low-voltage spark ignition caused by separating electrodes," in *Hazards, Prevention, and Mitigation of Industrial Explosions, 11th International Symposium on*, 2016.

[3] R. Shekhar, L. R. Boeck, C. Uber, and U. Gerlach, "Ignition of a hydrogen air mixture by low voltage electrical contact arcs." Submitted Manuscript, 2016.

[4] M. Ó Conaire, H. J. Curran, J. M. Simmie, W. J. Pitz, and C. K. Westbrook, "A comprehensive modeling study of hydrogen oxidation," *International journal of chemical kinetics*, vol. 36, no. 11, pp. 603–622, 2004.

[5] R. Shekhar and C. Uber, "Modelling of sparking contacts for hazardous area applications," in *Electrical Contacts (Holm), 2015 IEEE 61st Holm Conference on*, pp. 347–352, Oct 2015.

[6] I. B. Zeldovich and Akademiia nauk SSSR., *The Mathematical theory of combustion and explosions*. New York: Consultants Bureau, 1985.

[7] D. G. Goodwin, H. K. Moffat, and R. L. Speth, "Cantera: An object-oriented software toolkit for chemical kinetics, thermodynamics, and transport processes." `http://www.cantera.org`, 2016. Version 2.2.1.

[8] C. J. Sun, C. J. Sung, L. He, and C. K. Law, "Dynamics of weakly stretched flames: quantitative description and extraction of global flame parameters," *Combustion and flame*, vol. 118, no. 1, pp. 108–128, 1999.

[9] J. Bechtold and M. Matalon, "The dependence of the Markstein length on stoichiometry," *Combustion and Flame*, vol. 127, pp. 1906–1913, Oct. 2001.